Controls on mass balance sensitivity of maritime glaciers in the Southern Alps, New Zealand: The role of debris cover

Brian Anderson[1] and Andrew Mackintosh[1]

Received 17 April 2011; revised 2 November 2011; accepted 6 November 2011; published 7 January 2012.

[1] The "mass balance sensitivity" of a glacier provides a means for assessing its response to future warming and contribution to sea level rise. Many studies have concluded that the first-order control on mass balance sensitivity is climatic, where higher-precipitation (and less continental) glaciers are most sensitive while lower-precipitation (and more continental) glaciers are least sensitive. The Southern Alps in New Zealand experience a limited range of continentality (9–13 K) but strong gradients in precipitation (2.5–11 m a^{-1}). Using an energy balance model applied on a regional scale we find that the central Southern Alps glaciers are very sensitive to temperature change (1.9 m w.e. a^{-1} K^{-1}, with a range of −1.1 to −4.0 m w.e. a^{-1} K^{-1}) and that an 82% increase in precipitation is required to offset a 1 K warming. Spatial variations in mass balance sensitivity cannot be simply explained as a function of precipitation. Topographic effects are important, and we find that debris cover reduces mass balance sensitivity. Mass balance amplitude, which takes into account debris cover, hypsometry and other topographic characteristics, is a better predictor of mass balance sensitivity than precipitation. The mass balance gradient is almost as good a predictor indicating that hypsometry is not a necessary component of sensitivity calculations. Estimating mass balance sensitivity as a function of mass balance gradient allows for parameterizations of mass balance sensitivity based on glacier inventory data. This provides a simple and robust way to assess glacier mass balance sensitivity on a global scale, which may refine future predictions of valley glacier melt and its contribution to sea level rise.

Citation: Anderson, B., and A. Mackintosh (2012), Controls on mass balance sensitivity of maritime glaciers in the Southern Alps, New Zealand: The role of debris cover, *J. Geophys. Res.*, *117*, F01003, doi:10.1029/2011JF002064.

1. Introduction

[2] Of all glaciers and ice caps on Earth, maritime glaciers have the largest sensitivity to climatic changes, because they have high mass turnover [*Braithwaite et al.*, 2003; *Oerlemans and Fortuin*, 1992]. This high sensitivity, combined with short response times compared to ice sheets, means that maritime glaciers have lost significant mass in the past century [*Hoelzle et al.*, 2007] and will make a large contribution to sea level rise in the coming decades as the climate warms [*Raper and Braithwaite*, 2006]. Quantifying this contribution is difficult because we lack globally and regionally comprehensive information about glacier mass balance and, in some areas, even basic glacier inventory data. Several methods have been employed to account for the lack of mass balance data, including: interpolation or averaging from sparse glaciers for which mass balance sensitivity is known [*Cogley*, 2009; *Kaser et al.*, 2006; *Oerlemans et al.*, 2005], relating sensitivity to precipitation [*Oerlemans and Fortuin*, 1992; *Oerlemans et al.*, 2005], continentality (defined here as the difference between the mean temperature in the warmest and coolest month) [*De Woul and Hock*, 2005] or a combination of precipitation and continentality [*Hock et al.*, 2009].

[3] Calculations of glacier sensitivity are common for individual, well-known, glaciers [e.g., *Oerlemans*, 1992, 1997a; *Johannesson et al.*, 1995; *Braithwaite et al.*, 2003], but have rarely been undertaken on a regional basis [*Braithwaite and Raper*, 2007]. Calculating mass balance sensitivity regionally has the advantage that all glaciers, not just those well suited to mass balance measurement, are included. The Southern Alps, with its large precipitation gradients, provides an opportunity to assess how mass balance sensitivity varies in a single mountain range where glaciers experience annual precipitation totals in the range 2.5 to 11 m a^{-1} [*Henderson and Thompson*, 1999]. Many of these glaciers are debris covered, a characteristic which acts to reduce ablation on large, low-angle glacier tongues but has been given limited consideration in the analysis of glacier sensitivity even though it can have a significant impact on sea level rise estimates [*Arendt et al.*, 2002; *Berthier et al.*, 2010].

[4] Glaciers in the Southern Alps of New Zealand appear be particularly sensitive to climatic changes with estimates of the mass balance sensitivity, at between 1.3 and 2.0 m w.e. K^{-1} [*Oerlemans*, 1997b; *Anderson et al.*, 2006,

[1]Antarctic Research Centre, Victoria University of Wellington, Wellington, New Zealand.

0148-0227/12/2011JF002064

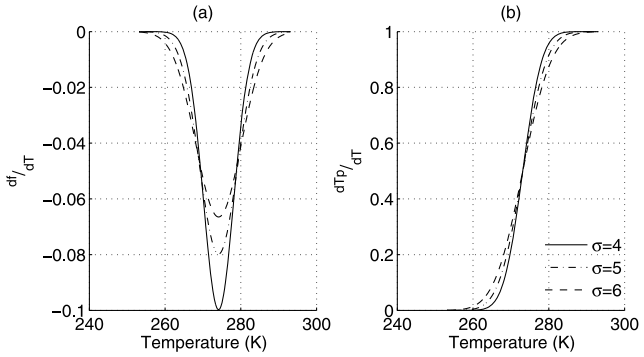

Figure 1. (a) The sensitivity of snow precipitation fraction to temperature from equation (2) and (b) the sensitivity of positive degree-day sums to temperature from equation (5). The shape of the curves changes depending on the value of the standard deviation of daily temperature within each month (σ).

2010], at the high end of global values [*Braithwaite et al.*, 2003]. As a result of this sensitivity, the ice mass in the Southern Alps has reduced due to warming since the mid-19th century [*Salinger et al.*, 1993], with estimates of the magnitude of loss varying between 30% [*Ruddell*, 1995] and 48% [*Hoelzle et al.*, 2007]. However, this ice loss has not been uniform with some glaciers, most notably Fox and Franz Josef glaciers, advancing significantly in response to mass balance changes since the late 1970s, while many other glaciers continue to down-waste and retreat [*Chinn*, 1999]. This contrasting behavior led to a view that glaciers that experience the highest precipitations rates, to the west of the main drainage divide, are sensitive to precipitation changes [*Hessell*, 1980; *Suggate*, 1952], while those to the east of the divide are sensitive to temperature changes [*Salinger et al.*, 1983]. However, mass balance modeling work [*Ruddell*, 1995; *Oerlemans*, 1997b; *Anderson et al.*, 2006; *Anderson and Mackintosh*, 2006; *Anderson et al.*, 2008] suggests that the converse is true, and that glaciers west of the divide are very sensitive to temperature changes, and not unusually sensitive to precipitation changes. The mass balance sensitivity of glaciers east of the divide has not been assessed but one would expect it to be lower as precipitation and mass turnover decrease, and continentality increases [*Braithwaite et al.*, 2003; *Oerlemans and Fortuin*, 1992; *Rasmussen and Conway*, 2005].

[5] Based on the existing literature, we hypothesize that the sensitivity of Southern Alps glaciers is high, and that there is a reduction in mass balance sensitivity from west to east as a result of decreasing precipitation and a slight increase in continentality. To test this hypothesis, we develop and apply an energy balance model on a regional scale to calculate the mass balance sensitivity of the ice mass in the Southern Alps of New Zealand. Specific questions that we explore are given below.

[6] 1. What is the range of mass balance sensitivity?

[7] 2. Which climatic and topographic characteristics control mass balance sensitivity?

[8] 3. Is there a simple and robust method for estimating mass balance sensitivity?

[9] Before applying this detailed energy balance model, we first present a simple analysis which forms the basis of our hypothesis that mass balance sensitivity is controlled by precipitation and continentality in this mountain range.

2. How is Mass Balance Sensitivity Influenced by Precipitation and Continentality?

[10] Mass balance is the sum of accumulation and ablation on the glacier surface. The sensitivity of accumulation c to changes in temperature is highest at the snow/rain threshold temperature. This can be illustrated through a simple analysis of the fraction of precipitation that falls as snow $f(T)$. We make use of the statistical relationship between daily and monthly temperature developed by *Braithwaite* [1985] which facilitates a semianalytical approach, and assume that temperatures within a given month m are normally distributed with mean T_m and standard deviation σ and take a snow/rain threshold of $T_{s,}$. In this case $f(T_m)$ can be written as

$$f(T_m) = 1 - \frac{1}{2}\left(1 + erf\,\frac{T_m - T_s}{\sigma\sqrt{2}}\right) \tag{1}$$

Differentiating with respect to temperature we find that the accumulation temperature sensitivity is greatest when the monthly temperature is at the snow/rain threshold temperature (Figure 1a):

$$\frac{df}{dT_m} = \frac{-1}{\sigma\sqrt{2\pi}}\mathrm{e}^{\left(\frac{Tm - Ts}{\sigma\sqrt{2}}\right)^2} \tag{2}$$

Assuming that precipitation P falls uniformly throughout the year we can describe the accumulation sensitivity at a point as

$$\frac{dc}{dT} = \frac{P}{12}\sum_{m=1}^{12}\frac{df}{dT_m} \tag{3}$$

demonstrating that the sensitivity of accumulation to temperature is proportional to the annual accumulation on a glacier.

[11] Ablation sensitivity is more difficult to resolve analytically. To simplify matters a degree-day approach can be used to illustrate the temperature dependence of ablation sensitivity. The positive temperature sum T_p , which is assumed to be linearly related to ablation through a degree-day factor k, can written as [*Calov and Greve*, 2005]

$$T_p = \sum_{m=1}^{12}\frac{\sigma}{\sqrt{2\pi}}\exp\left(\frac{-T_m^2}{2\sigma^2}\right) + \frac{T_m}{2}erfc\left(-\frac{T_m}{\sqrt{2}\sigma}\right) \tag{4}$$

Differentiating with respect to temperature we find that the temperature sensitivity of the degree-day sum approaches 1 K d^{-1} when the monthly mean temperature exceeds a value which depends on σ (Figure 1b).

$$\frac{dT_p}{dT_m} = \frac{1}{2}erfc\left(\frac{-T_m}{\sqrt{2}\sigma}\right) \tag{5}$$

Assuming we can write the annual ablation sensitivity as the sum of monthly sensitivities, the annual ablation sensitivity is

$$\frac{da}{dT} = k\sum_{m=1}^{12}\frac{dT_p}{dT_m} \tag{6}$$

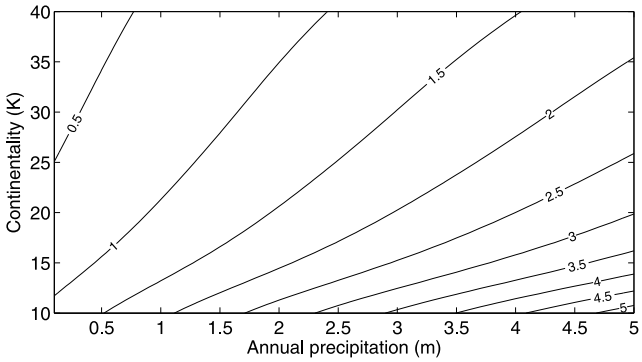

Figure 2. The idealized relationship between continentality, precipitation, and mass balance temperature sensitivity at the ELA. Sensitivity is the sum of accumulation sensitivity (equation (3)) and ablation sensitivity (equation (6)). Sensitivity to temperature is contoured, with contour units of m w.e. K^{-1} a^{-1}. The values are calculated for a degree-day factor k = 5 mm w.e. K^{-1} a^{-1} and snow/rain temperature threshold T_s = 274 K.

where k is the degree-day factor. Where the monthly temperature $T_m \ll 0$, ablation sensitivity is zero, and where $T_m \gg 0$ sensitivity of the degree-day sum is limited to 1 K d^{-1}.

[12] While estimating mass balance sensitivity for an entire glacier requires equations (3) and (6) to be integrated over the glacier surface, there is a close relationship between mass balance sensitivity at the equilibrium line altitude (ELA) and overall sensitivity [*Braithwaite and Raper*, 2007], and so we assess sensitivity at the ELA. The difference in ablation sensitivity between continental and maritime glaciers occurs because the summer temperature at the ELA is lower in continental climates than maritime climates [*Ohmura et al.*, 1992] and ablation is less sensitive at lower temperatures (Figure 1b). These relationships are summarized in Figure 2, which shows the dependence of mass balance sensitivity at the ELA on continentality and precipitation, assuming a sinusoidal variation for

$$T_m = \frac{C}{2}\sin\left(\frac{2\pi m}{12}\right) + T_{mean} \tag{7}$$

where C is continentality. The mean annual temperature T_{mean} is taken from a linear relationship (r^2 = 0.38) between summer temperature at the ELA of many glaciers [*Ohmura et al.*, 1992] and, following *Braithwaite* [2008], continentality estimated at the 64 of these glaciers which have corresponding temperature data in the gridded climatology of *New et al.* [2002].

[13] Note that rainfall has negligible influence on ablation, only supplying a few percent of the energy available for melt even in high-precipitation environments [*Anderson et al.*, 2010]. This simple analysis also neglects the feedback between melt rates and albedo which can be significant [*Oerlemans*, 2001].

[14] Overall, this analysis demonstrates that glaciers with high precipitation rates and low continentality will experience high mass balance sensitivity. We now test this hypothesis in the Southern Alps of New Zealand, where a steep gradient in precipitation across the glacierized part of the mountain range (from 2.5 to 11 m a^{-1}) coincides with a smaller gradient in continentality (9–13 K). In this climatic setting, we expect that a gradient of mass balance temperature sensitivity will occur, decreasing from high values in the west to lower values to the east.

3. Study Area

[15] The central portion of the Southern Alps (Figure 3) contains most of the glacier ice in New Zealand. The 38 × 40 km model domain contains 35% of glacier area and the four largest glaciers which together account for ~45% of ice volume [*Chinn*, 2001]. The crest of the mountain range within the domain varies from 2150 to 3764 m above sea level, with the drainage divide located only 27 km from the Tasman Sea coast. The region experiences a very strong precipitation gradient, with annual rates of ~3 m at the Tasman Sea coast, increasing to 10–12 m west of the main divide, and decreasing exponentially to ~1 m at the southwest margin of the model domain [*Henderson and Thompson*, 1999]. There are very few climate stations in this area and there are still significant climatic uncertainties, especially in the magnitude of precipitation at high elevations.

[16] Glaciers in the domain show a wide range of morphology, from steep glaciers covering a large elevation range (Fox and Franz Josef glaciers), small alpine glaciers (e.g., Tewaewae/Stocking and Reay glaciers) and large, low-angle valley glaciers (e.g., Tasman and Murchison glaciers). Many of these glaciers have significant surface debris cover, with Tasman Glacier, the largest in the Southern Alps, being ~30% debris covered. While the best known glaciers located to the west, Fox and Franz Josef have virtually no surface debris and the best known glacier located to the east, Tasman, has a large debris cover, there is no systematic relationship between debris cover and precipitation amount. For example Burton Glacier, on the western flanks of the mountain range, has ~55% debris cover.

4. Methodology

4.1. Input Data

[17] For the detailed energy balance model used in this study, daily data for several climatic variables are derived from three sources. For relative humidity and solar radiation, gridded climate data sets, available at a daily temporal scale and a 0.05° spatial scale (which corresponds to ~5 km in the study area), are created by a trivariate spline interpolation from long-term climate station data at a large number of sites [*Tait et al.*, 2006]. The interpolation is for all of New Zealand and the number of stations used depends on data availability, but is approximately 500 for relative humidity and 100 for solar radiation. As glaciers in the Southern Alps generally occur on a smaller scale than the relatively coarse spatial scale of the climate grids, the data are resampled onto a finer grid using bilinear interpolation.

[18] Wind speed data in these gridded climate data sets have large temporal and spatial artifacts and were not used directly in this study. Instead, the mean gridded wind speed between 2000 and 2010 was compared against NCEP reanalysis wind speed [*Kalnay et al.*, 1996] at the 850 hPa level. The frequency distribution of the two data sets is similar, except at low wind speeds which are not used by the

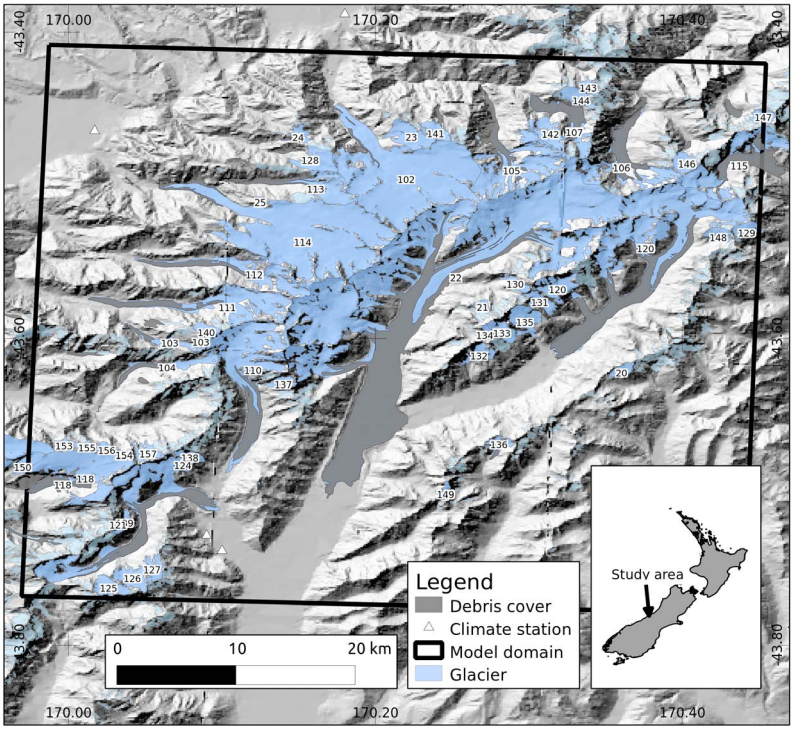

Figure 3. The central part of the Southern Alps considered in this study includes Franz Josef, Fox, and Tasman glaciers for which some mass balance measurements exist. Other selected glaciers, >0.5 km^2 in surface area, have identifying numbers which correspond with the glacier names in Table 4. Data from 22 climate stations (many of which are outside the model domain) are used to interpolate temperature and precipitation. Inset map shows the location of the study area in New Zealand.

model, and so the reanalysis wind speed was reduced by a factor of 2.9 (reflecting the relative median wind speeds in the reanalysis data and gridded data set) and applied uniformly across the domain. This method resulted in an improved spatial distribution of mass balance and avoided the temporal artifacts in the gridded data set.

[19] The temperature fields in the gridded climate data sets were also deemed unsuitable for this study because they were based on lowland climate data and poorly represented measured temperature at high elevation. Instead, temperature was separately interpolated for the mountainous regions using 31 long-term climate records from the 22 closest sites inside and surrounding the model domain, collected by the National Institute of Water and Atmosphere (Figure 3). Temperature interpolation was carried out by taking the daily temperature measured at each site, using a constant lapse rate to calculate a sea level temperature, and interpolating this "reference temperature" across the model domain. The temperature at any grid cell was calculated by using the same lapse rate (Table 1), the reference temperature at the grid cell location and the elevation of that grid cell.

[20] Precipitation on the model grid was calculated at daily resolution using a combination of measured rainfall and a mean annual precipitation surface interpolated from rain gauge measurements using a spline [*Stuart*, 2011]. This surface includes many stations in mountainous areas that had not previously been included in precipitation interpolations. For each day, the proportion of mean annual precipitation at each station was interpolated across the model grid, and this proportional value was then multiplied by the mean annual precipitation surface to calculate the precipitation at each grid cell. The method returned the measured daily values at locations where rainfall is measured. Away from measurement sites the interpolated daily precipitation is controlled by nearby stations and sums to annual values which are consistent with the mean annual surface (although not identical as precipitation totals vary from year to year).

4.2. Topographic Data

[21] A digital elevation model (DEM) is used to provide the surface elevation throughout the model domain. It is photogrammetrically derived from stereo image pairs taken in 1986 as part of the national topographic New Zealand Map Series 260 (NZMS 260), and the manually drawn contours have subsequently been digitized and interpolated into a 25 m resolution DEM. The DEM is resampled to 100 m for use by the model. An ice mask is derived from the perennial snow and ice vector layer from the same mapping series and is used to create a grid at the same 100 m resolution. Glacier debris cover is derived from the same data set.

4.3. Model Description

4.3.1. Ablation Model

[22] The energy balance model used in this study is identical to that used by *Anderson et al.* [2010] and is described only briefly here. An energy balance model is preferred over a temperature index model in this sensitivity analysis because an energy balance model explicitly calculates all energy

Table 1. A Summary of the Values of Parameters Used to Calculate Model Input Data and Mass Balance

Parameter	Symbol	Value	Source
		Climatic Variations	
Temperature lapse rate	$\frac{dT}{dz}$	-0.005 K m^{-1}	*Anderson et al.* [2006]
		Shortwave Radiation	
Albedo of fresh snow	α_{snow}	0.9	*Oerlemans and Knap* [1998]
Albedo of firn	α_{firn}	0.53	*Oerlemans and Knap* [1998]
Albedo of ice	α_{ice}	0.36	*Oerlemans and Knap* [1998]
Albedo characteristic depth	d_c	11 mm w.e.	*Oerlemans and Knap* [1998]
Albedo characteristic time scale	t_c	21.9 days	*Oerlemans and Knap* [1998]
		Turbulent Heat Fluxes	
Roughness parameter for ice	z_{ice}	0.004 m	Tuned to Franz Josef ablation measurements 2000–2002
Roughness parameter for snow	z_{snow}	0.0004 m	Tuned to Franz Josef ablation measurements 2000–2002
		Accumulation	
Snow/rain temperature threshold	T_s	274 K	*Barringer* [1989], *Moore and Owens* [1984], *Anderson et al.* [2006]

sources that contribute to ablation whereas the temperature index model assumes that all ablation is related to temperature, and can hence overestimate temperature sensitivity [*Oerlemans*, 2001]. The model calculates the energy available for melt on snow and ice surfaces:

$$Q_m = I(1-\alpha) + L_{out} + L_{in} + Q_H + Q_E + Q_R + Q_G \quad (8)$$

where Q_m is the energy available for melt, I the incoming short-wave radiation, α the surface albedo, L_{out} the outgoing longwave radiation, L_{in} the incoming longwave radiation, Q_H the sensible heat flux, Q_E the latent heat flux, Q_R the heat flux supplied by rainfall, and Q_G the heat flux conducted from the ice. The various components of the energy balance are calculated using climatic and topographic data.

[23] Incoming shortwave radiation I is derived using a diffuse and direct component [*Oerlemans*, 1992], from calculated radiation at the top of the atmosphere (I. Eisenman and P. Huybers (2006), Paleo insolation Matlab function, 2006, accessed 23 June 2008; available at http://www.ncdc.noaa.gov/paleo/pubs/huybers2006b/huybers2006b.html). A cloudiness value is inferred from measured incoming solar radiation (from the gridded climate data set [*Tait et al.*, 2006]) to partition direct and diffuse components. The spatial distribution of shortwave radiation is calculated using topographic shading [*Corripio*, 2003]. Surface albedo controls the magnitude of absorbed and reflected shortwave radiation, calculated using the method of *Oerlemans and Knap* [1998] where the albedo depends on the length of time since the last snowfall and a background albedo distribution which reflects the transition from dominant snow cover to ice cover as the melt season progresses. This scheme has been found to correspond well to albedo measurements at nearby Brewster Glacier [*Anderson et al.*, 2010].

[24] Outgoing longwave radiation L_{out} is calculated using the Stefan-Boltzmann law, while incoming longwave radiation L_{in} is split into an atmospheric and terrain component according to the sky view of each point on the grid. The emissivity and emission temperature of these components are different.

[25] Turbulent heat fluxes Q_H and Q_E, which make up half or more of the energy available for melt in maritime environments, are calculated using a bulk aerodynamic approach, with a variable roughness length for snow and ice surfaces. The Richardson stability criterion is used to correct the exchange coefficients for stable conditions [*Hock*, 2005].

[26] Precipitation heat flux Q_R is calculated assuming that precipitation is at air temperature. Subsurface heat fluxes are neglected which, while not strictly correct, is expected to have little influence on the mass balance calculation on temperate glaciers which have a limited annual temperature range and do not contain significant amounts of snow and ice below 0°C [*Oerlemans*, 1992]. The ground heat flux is set at $Q_G = 1$ Wm^{-2} [*Neale and Fitzharris*, 1997].

4.3.2. Debris Cover

[27] Large parts of some glaciers in the Southern Alps are covered with a varying thickness of debris, totaling 92 km^2, or 8% of the total glacier area. This debris is largely derived from rockfall from the steep and rapidly uplifting mountain sides. Debris cover of Southern Alps glaciers has been mapped as part of the NZMS260 national topographic mapping series. Only thick debris cover has been mapped, rather than "dirty ice," and so the mapped debris cover will have the effect of decreasing ablation [*Paterson*, 1994]. While the increased ablation caused by dirty ice may be of local importance, it is likely to be insignificant on a regional scale, because debris cover has retarded the overall response of New Zealand glaciers to 20th century climate warming [*Warren and Kirkbride*, 2003]. The Tasman Glacier has the most extensive and best studied debris cover, generally varying in thickness between 0 and 3 m [*Kirkbride*, 1989]. Reduction in ablation under 1.1 m of debris on the Tasman Glacier was estimated at 93% [*Purdie and Fitzharris*, 1999], and *Kirkbride* [1989] calculated a reduction in ablation of 89% under debris cover. There are insufficient data on either the distribution of debris thickness or the relationship between debris thickness and ablation suppression to calculate ablation under debris cover with any rigor. Hence, ablation calculated by the energy balance model is reduced by 90% where there is debris cover and where any snow accumulation on top of the debris has melted.

4.3.3. Accumulation Model

[28] Snow accumulation is modeled from the precipitation value within each grid cell by using a simple temperature threshold to discriminate rain from snow. The threshold T_s is set at 274 K, a value used in other snow modeling studies in New Zealand [*Moore and Owens*, 1984; *Barringer*, 1989;

Table 2. A Summary of the Mass Balance Data Used in This Study

Purpose	Glacier	Balance Year	Number of Observations	e_{rms} (m w.e.)	r^2
Tuning	Franz Josef Glacier[a]	1 April 2000 to 31 March 2002	455	0.38	0.61
Testing	Franz Josef Glacier[a]	1 April 2002 to 31 March 2010	288	0.62	0.48
Testing	Tasman Glacier[b]	1 April 2007 to March 2009	65	0.67	0.55
Testing	Fox Glacier[c]	1 April 2007 to March 2010	73	0.52	0.57

[a]*Anderson et al.* [2006] and later measurements.
[b]Data collected by Heather Purdie, 2007–2008.
[c]Data collected by Fox Glacier Guides, 2007–2010.

Anderson et al., 2006, 2010]. The sensitivity of model results to this choice is tested later. Snow thickness is truncated at a maximum value (Table 1) to avoid build up of excessive snow thickness in glacier accumulation areas, reflecting the process of firnification.

[29] A summary of the parameter values used in the climate data interpolation, energy balance and accumulation models is given in Table 1.

4.4. Mass Balance Data

[30] A data set of point mass balance measurements has been established in the last decade, with ~800 individual mass balance measurements from Franz Josef Glacier [*Anderson et al.*, 2006], and records of point mass balance from the Tasman Glacier (H. Purdie, personal communication, 2008) and Fox Glacier (Fox Glacier Guides, personal communication, 2010). While these measurements are insufficient to calculate total mass balance for any glacier, they are used for model calibration and testing.

5. Results

5.1. Model Calibration and Evaluation

[31] The baseline comparison for model performance is with measured mass balance data. To compare modeled and measured mass balance, two metrics are used: the root mean standard error to measure the quality of fit between measured and modeled mass balance:

$$e_{rms} = \frac{\sqrt{\sum_{1}^{n} (o_i - m_i)^2}}{\sqrt{n}} \tag{9}$$

where o_i and m_i are observed and modeled values at the same location and n is the number of observations, and the coefficient of determination to estimate the proportion of variability that is explained by the model:

$$r^2 = 1 - \frac{e_{rms}}{2\sigma} \tag{10}$$

where σ is the standard deviation of the measured mass balance. The model is calibrated against measured mass balance at Franz Josef Glacier using data collected between 2000 and 2002 [*Anderson et al.*, 2006]. There are $n = 455$ individual mass balance measurements during this time, heavily skewed toward ablation measurements. As the least well constrained parameters in the model are the turbulent heat flux coefficients z_{ice} and z_{snow}, these were varied to the values in Table 1 to get the best fit between modeled and measured data for this period. The sensitivity of the model to these and other parameters is evaluated in section 5.2.

[32] The performance of the model is tested against an independent set of mass balance data collected between 2002 and 2010 at three different glaciers (Table 2). The results of this exercise show that, as expected, the model simulates mass balance best during the tuning period. The validation period on each of the three test glaciers indicates that the simulation is good at Franz Josef Glacier (the calibration site) and Fox Glacier. The mass balance simulation at Tasman Glacier has the highest e_{rms} value, but the coefficient of determination r^2 is adequate at 0.55 (Table 2 and Figure 4).

5.2. Model Sensitivity

[33] As the model has a number of parameters that are tuned or that have an unknown level of uncertainty, it has been run a number of times with different parameter values to test the sensitivity of the model to its parameters. The parameter values are chosen conservatively to cover the range of accepted values. Where there are no accepted values (for example the turbulent transfer coefficients) the values are tested with a 50% increase and decrease relate to the control run. The results of this sensitivity study are presented in terms of the overall mass balance of all glacier areas in the model domain (Table 3), and the fit between measured and modeled mass balance, as measured by the coefficient of determination r^2 and the absolute root mean standard error e_{rms}.

[34] The model is very sensitive to temperature lapse rate, with variations of +/−0.001 K m^{-1} resulting in a total mass balance of −4.2 and +2.4 m w.e. a^{-1}. Changes of +/−1 K in the snow/rain temperature threshold results in total mass balance of −1.3 and +1.1 m w.e. a^{-1}. These results are in accordance with the results of other studies in a similar maritime environment [*Anderson and Mackintosh*, 2006; *Anderson et al.*, 2010]. Variations in other parameters have a smaller influence (Table 3).

[35] The sensitivity analysis also reveals that, according to the two metrics of model performance used, there are a number of parameter choices which give a good fit to the measured data but result in different overall mass balance. There is a problem of equifinality here, which in this case means that two or more sets of model parameters result in an acceptable representation of mass balance. This is most pronounced with parameters that influence accumulation such as the temperature lapse rate, the snow/rain temperature threshold T_s, or the precipitation surface used. This issue largely results from a relative lack of accumulation measurements on these glaciers to constrain the accumulation calculation with. To address this issue we select the parameter choices which (1) fit the mass balance data at least as well as the control run and (2) result in a significantly

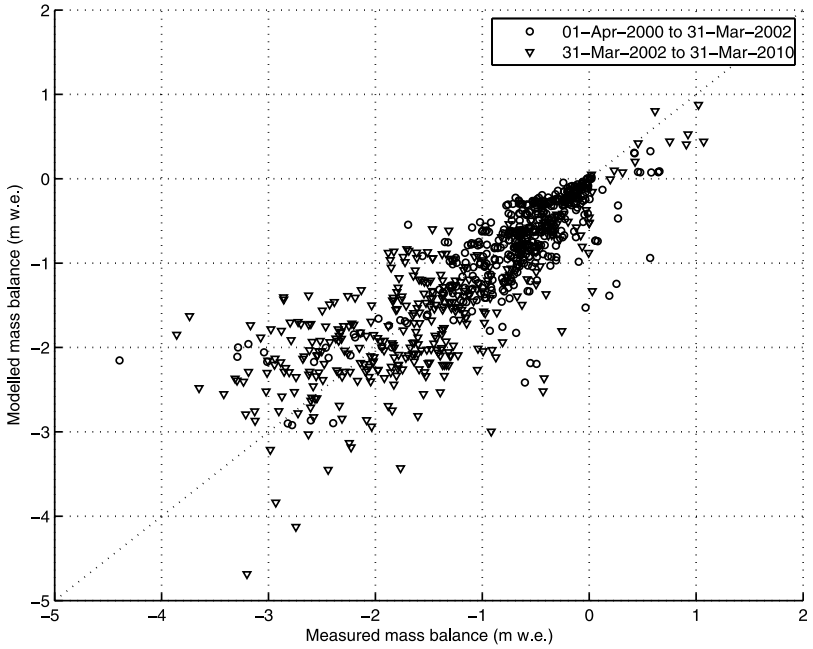

Figure 4. Measured and modeled mass balance at Franz Josef Glacier during the calibration period (1 April 2000 to 31 March 2002) and at Franz Josef, Fox, and Tasman glaciers during the validation period (31 March 2002 to 31 March 2010).

different mass balance output. These selected parameters and values are dT/dz = −0.006 K m^{-1}, α_{snow} = 1.0, t_c = 33 days, z_{ice} = 2 mm, z_{snow} = 0.2 mm, and T_s = 275 K. Some of these parameter values could be rejected for other reasons, for example α_{snow} = 1.0 is physically unrealistic and dT/dh = −0.006 K m^{-1} results in a overall mass balance that is unrealistically positive. However, it is instructive to see what impact these parameter choices have on the overall mass balance sensitivity results.

[36] The full suite of model sensitivity runs is conducted for each of these selected parameters and values. The results (Figure 5) show that most of the parameters have little influence on the mass balance sensitivity, even though they have a moderate influence on the mass balance itself (Table 3). The exceptions are the snow/rain threshold temperature T_s = 275 K and the temperature lapse rate dT/dz = −0.006 K m^{-1}. These two parameter choices result in changes to the overall mass balance of more than 1 m w.e. a^{-1} (Table 3) and decreases the temperature sensitivity by a mean of 34% for the larger lapse rate, and 10% for the higher snow/rain threshold temperature (Figure 5). The precipitation sensitivity is increased by a mean of 20% for the lapse rate change and 17% for the snow/rain threshold temperature change. We conclude that for all parameters the patterns and relative order of mass balance sensitivity between glaciers does not change even with large changes in the overall values of simulated mass balance.

5.3. Mass Balance Variations

[37] The mass balance reconstruction for a number of large glaciers in the Southern Alps indicates that, while mass balance variations generally show the same temporal pattern for each glacier (Figure 6), there are some significant deviations from that pattern as a result of varying glacier sensitivity and state of balance. These calculations are all carried out on glaciers of fixed geometry and hence result in a "reference surface mass balance" which directly reflects the climatic component of mass balance variations [*Elsberg et al.*, 2001].

[38] The selection of glaciers plotted shows a distinct difference between glaciers which are debris free and have a short response time (Fox and Franz Josef) and the remainder of the large glaciers which have low-gradient tongues and

Table 3. Deviation of Mass Balance From Standard Run for Different Model Parameter Values[a]

Parameter and Value	e_{rms} (m)	r^2	Mass Balance (m w.e. a^{-1})
Standard	0.46	0.75	−0.31
dT/dh = −0.004 K m^{-1}	0.64	0.52	−4.23
dT/dh = −0.006 K m^{-1}	0.42	0.79	2.37
Henderson and Thompson [1999] precipitation	0.46	0.74	−0.86
α_{snow} = 0.8	0.47	0.73	−0.59
α_{snow} = 1.0	0.46	0.75	−0.09
α_{firn} = 0.6	0.51	0.69	−1.38
α_{firn} = 0.5	0.49	0.72	−1.85
α_{ice} = 0.3	0.47	0.74	−0.38
α_{ice} = 0.4	0.51	0.69	−0.20
d_c = 5.5 mm	0.46	0.75	−0.29
d_c = 16.5 mm	0.46	0.75	−0.33
t_c = 11 days	0.48	0.73	−0.66
t_c = 33 days	0.46	0.75	−0.09
z_{ice} = 2 mm	0.46	0.75	−0.10
z_{ice} = 6 mm	0.50	0.70	−0.47
z_{snow} = 0.2 mm	0.46	0.75	−0.17
z_{snow} = 0.6 mm	0.47	0.74	−0.41
T_s = 273 K	0.49	0.71	−1.62
T_s = 275 K	0.44	0.77	0.76

[a]The values of e_{rms}, r^2, and mass balance are for the complete model period 2000–2010 and hence include both calibration and testing data sets.

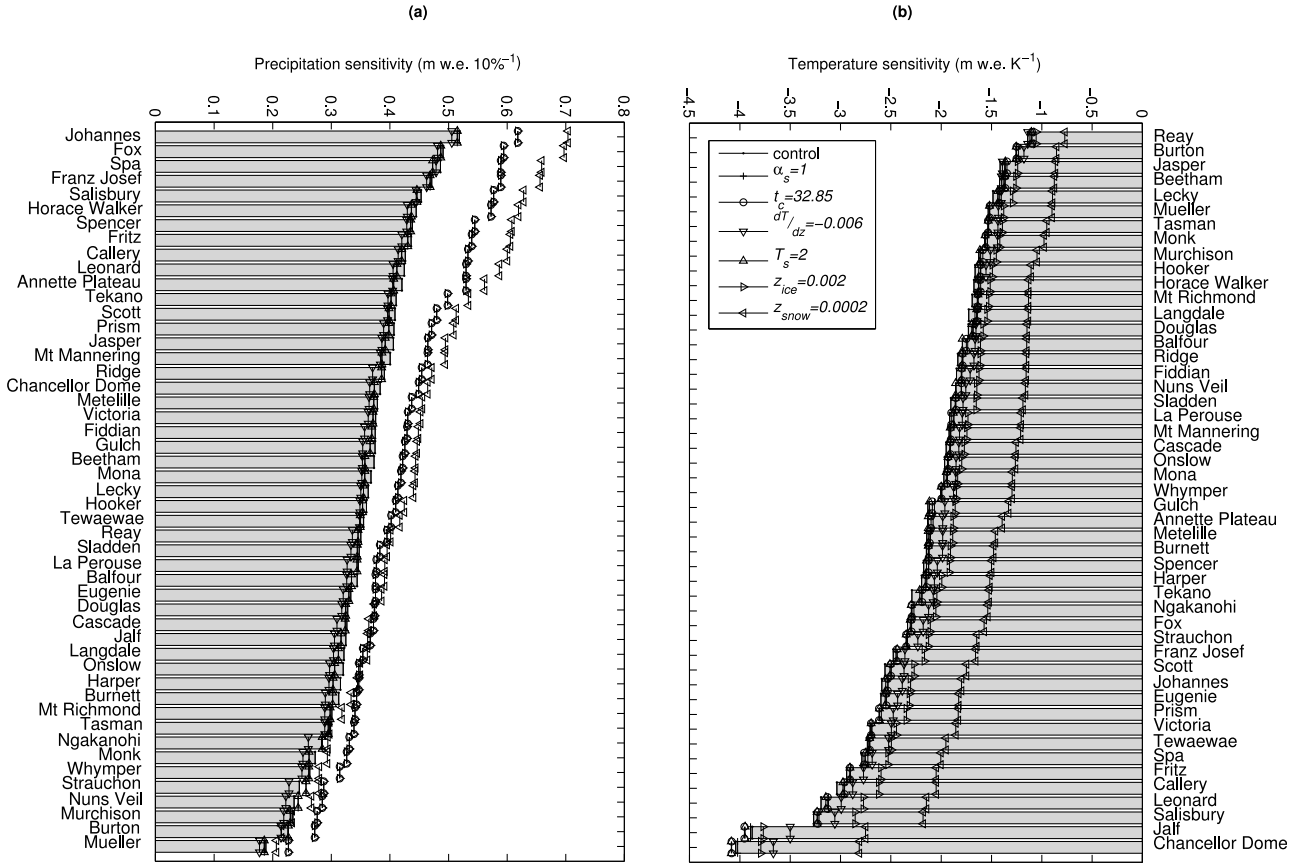

Figure 5. Mass balance sensitivity to (a) temperature and (b) precipitation changes is ordered by the magnitude of the sensitivity in the control run (gray bars). The variability of the sensitivity resulting from different parameter choices is indicated by black lines with different markers for each parameter/value combination.

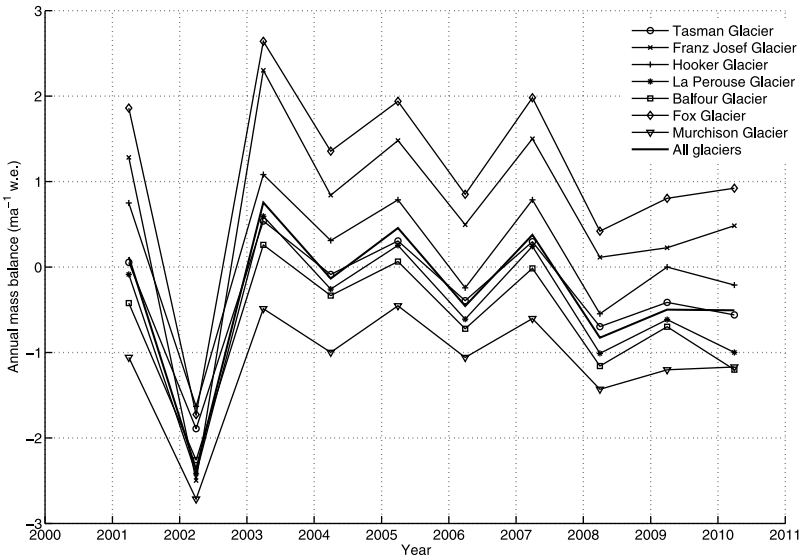

Figure 6. Modeled variations in mass balance 2000–2010. There is a clear difference between Fox and Franz Josef glaciers, which were close to their 20th century minimum length in 1986, and the other glaciers which are all debris covered and were in various stages of lake-calving retreat in 1986.

significant debris cover. Fox and Franz Josef glaciers had a several positive mass balance years during the period which is not surprising given that both glaciers have increased their length since 1986, meaning that ablation has been underestimated in the model period 2000–2010. For the debris covered glaciers, the generally negative mass balance calculated indicates that they are out of balance with the present-day climate and there is no systematic difference in the state of balance of glaciers to the west of the main divide (La Perouse and Balfour glaciers) and those east of the main divide (Hooker and Murchison glaciers).

5.4. Mass Balance Sensitivity

[39] The overall sensitivity of the volume of Southern Alps ice in the model domain to climatic changes is calculated by taking the mean difference between the total mass balance for the 10 year period 2000–2010 (-0.31 m w.e. a^{-1}) and the mass balance when a $+/-1$ K temperature change is imposed on the model. The results imply an overall sensitivity of -1.9 m w.e. a^{-1} K^{-1} for temperature changes, and a sensitivity of 0.34 m w.e. for a 10% change in precipitation. An experiment where the temperature is increased by 1 K and the precipitation is increased until the overall mass balance equals that of the control run indicates that a 82% precipitation increase is required to offset a 1 K warming.

[40] While mass balance sensitivity may be easily calculated for a single glacier, it requires that the geographic extent of that glacier be known, so that sensitivity at each point can be integrated over the glacier as a whole. The New Zealand glacier inventory [*Chinn*, 1989, 2001] has point location and topographic descriptions of all glaciers in New Zealand but as yet there is no database of glacier outlines for the Southern Alps. For 53 selected glaciers in the model domain (with area > 0.5 km^2) the glacier outline has been derived from the perennial snow and ice layer in the national topographic mapping series (NZMS 260; 1986) and clipped into individual glacier entities. Key geometric and climatic data from these glaciers are presented in Table 4. Mass balance sensitivity for glaciers in this domain has only been previously calculated on Franz Josef Glacier [*Oerlemans*, 1997b; *Anderson et al.*, 2006] at -1.3 and -1.6 m w.e. K^{-1}, less that the -2.5 m w.e. K^{-1} calculated here. This difference is attributed to the different precipitation values in the accumulation area used in those studies ($\sim$5 m a^{-1}) compared to the values of $\sim$10 m a^{-1} used in this study. This latter value is based on updated interpolations from many low-elevation rain guages [*Stuart*, 2011], is consistent with recent ground-penetrating radar studies of the snowpack at the end of winter [*Kees*, 2011], and previous regional estimates of precipitation [*Henderson and Thompson*, 1999].

5.5. Relationship Between Mass Turnover and Mass Balance Sensitivity

[41] The quantity "mass balance amplitude" is used as a direct measure of mass turnover [*Dyurgerov and Meier*, 2000] and is calculated as

$$b_a = \frac{b_w - b_s}{2} \tag{11}$$

where b_w is the winter balance (usually positive) and b_s the summer balance (usually negative).

[42] For the Southern Alps sensitivity data set, there is a strong relationship between mass balance amplitude and both temperature sensitivity (r^2 = 0.67; Figure 7a) and precipitation sensitivity (r^2 = 0.57; Figure 8a). Another method of parameterizing mass turnover is using the mass balance gradient, which is the change in mass balance with elevation. There is a strong relationship between mass balance gradient, calculated from model output, and temperature sensitivity (r^2 = 0.61; Figure 7b) but a weaker relationship for precipitation sensitivity (r^2 = 0.26; Figure 8b).

[43] Mass balance amplitude takes into account all topographic and climatic influences on sensitivity. Mass balance gradient neglects hypsometry, but still takes into account slope, accumulation rate, ablation rate and influence of debris cover on melt.

5.6. Relationship Between Climate, Topography, and Mass Balance Sensitivity

[44] Temperature sensitivity of mass balance is only weakly related to precipitation (r^2 = 0.26; Figure 7c) and continentality (r^2 = 0.18; Figure 7d). Similarly, precipitation sensitivity of mass balance is only weakly related to precipitation (r^2 = 0.24; Figure 8c) and continentality (r^2 = 0.11; Figure 8d). There is a limited range of continentality in the Southern Alps which may explain the lack of a clear relationship.

[45] Several topographic characteristics were tested against mass balance sensitivity: (1) mean slope because low-angle glaciers are thought to be more sensitive [*Oerlemans*, 1989], (2) various elevation parameters because glaciers that have a large elevation range or descend to low elevations are thought to be more sensitive [*Furbish and Andrews*, 1984; *Oerlemans*, 2001], and (3) debris cover because debris covered glaciers should be less sensitive to temperature change.

[46] The influence of debris cover on mass balance sensitivity has not been discussed before, but it follows that because the ablation is reduced under thick debris cover, the sensitivity of ablation to temperature changes will also be reduced.

[47] The only one of these topographic glacier characteristics that showed any relationship with mass balance sensitivity, relative to either temperature or precipitation changes, is debris-covered area with r^2 = 0.50 for temperature sensitivity (Figure 7e) and r^2 = 0.43 for precipitation sensitivity (Figure 8e).

6. Discussion

6.1. Regional Energy Balance Modeling

[48] The results of this study are predicated on the ability to simulate mass balance on a regional scale using an energy balance model. In particular there is an assumption about the transferability of both model parameters and input data, in both space and time [*MacDougall et al.*, 2010]. Model testing has indicated that the parameters and climate interpolation used at Franz Josef Glacier (the calibration site) adequately simulate the mass balance at two other glaciers within the model domain (Tasman Glacier and Fox Glacier). During the testing period the mass balance model simulated mass balance observations at Fox Glacier with a similar degree of accuracy as at the calibration site of Franz Josef Glacier (Table 2). However, the mass balance measurements

Table 4. Physical Characteristics and Mass Balance Sensitivity of a Selection of Glaciers in the Southern Alps

Glacier	ID	Area[a] (km^2)	Debris Area[a] (%)	Mean Precipitation[b] ($m\ a^{-1}$)	Mean Continentality[c] (K)	Mass Balance Amplitude (m w.e.)	Mass Balance Gradient ($mm\ m^{-1}$)	Temperature Sensitivity[d] ($m\ w.e.\ K^{-1}$)	Precipitation Sensitivity ($m\ w.e.\ (10\%)^{-1}$)
Annette Plateau	127	1.3	0	4.6	12.5	2.2	7.4	−2.1	0.42
Balfour Glacier	112	7.7	23	10.5	10.4	2.0	4.1	−1.8	0.34
Beetham Glacier	130	0.8	0	6.5	10.4	2.1	6.6	−1.4	0.37
Burnett Glacier	132	1.1	0	5.5	10.8	2.1	8.1	−2.1	0.31
Burton Glacier	107	5.1	56	10.2	9.8	1.6	5.3	−1.3	0.23
Callery Glacier	143	0.8	0	10.6	9.7	2.9	12.6	−3.0	0.43
Cascade Glacier	131	1.1	0	5.9	10.6	2.1	9.7	−2.0	0.33
Chancellor Dome	25	0.2	0	10.7	9.8	3.1	14.5	−4.0	0.38
Douglas Glacier	118	11.1	16	7.2	11.6	2.1	3.2	−1.7	0.33
Eugenie Glacier	138	0.8	0	6.2	11.9	2.6	11.1	−2.6	0.33
Fiddian Glacier	157	1.0	0	6.9	11.7	2.2	8.4	−1.8	0.37
Fox Glacier	114	37.4	2	10.5	10.1	2.9	9.1	−2.3	0.49
Franz Josef Glacier	102	34.5	1	10.6	9.6	3.0	6.8	−2.5	0.47
Fritz Glacier	128	2.6	0	10.5	9.5	3.0	14.7	−2.9	0.44
Gulch Glacier	103	2.5	12	10.0	10.7	2.4	10.3	−2.1	0.37
Harper Glacier	148	1.1	0	5.5	11.2	2.0	9.5	−2.2	0.32
Hooker Glacier	110	18.7	18	7.8	11.4	2.0	8.2	−1.7	0.36
Horace Walker Glacier	119	1.0	0	8.6	11.3	2.8	4.3	−1.7	0.44
Jalf Glacier	24	0.9	0	9.3	9.3	2.9	15.6	−3.9	0.32
Jasper Glacier	154	0.3	0	7.1	11.6	2.2	5.7	−1.4	0.41
Johannes Glacier	142	2.4	0	10.3	9.7	2.9	10.7	−2.6	0.52
La Perouse Glacier	111	11.0	19	10.2	10.6	2.2	4.1	−1.9	0.35
Langdale Glacier	21	0.4	0	6.4	10.4	2.3	5.7	−1.7	0.32
Lecky Glacier	133	1.4	0	5.7	10.6	2.0	6.7	−1.5	0.36
Leonard Glacier	144	1.6	0	10.6	9.7	2.9	12.6	−3.2	0.42
Metelille Glacier	126	2.0	0	4.6	12.5	2.1	7.3	−2.1	0.38
Mona Glacier	137	0.8	0	7.1	11.5	2.4	9.3	−2.0	0.37
Monk Glacier	136	1.0	22	3.2	11.4	1.7	0.6	−1.6	0.27
Mt Mannering	146	1.4	0	7.4	10.6	2.3	8.1	−1.9	0.40
Mt Richmond	129	1.2	0	5.3	11.3	1.9	7.1	−1.7	0.30
Mueller Glacier	121	16.7	28	5.6	12.1	1.7	2.9	−1.5	0.19
Murchison Glacier	120	40.7	26	5.8	10.8	1.7	3.3	−1.6	0.23
Ngakanohi Glacier	139	0.7	0	5.6	12.2	2.1	9.1	−2.3	0.28
Nuns Veil Glacier	149	0.1	0	2.5	11.9	1.8	4.3	−1.9	0.24
Onslow Glacier	135	2.5	0	5.7	10.6	2.2	8.5	−2.0	0.32
Prism Glacier	156	0.3	0	7.7	11.5	2.6	12.9	−2.6	0.41
Reay Glacier	134	0.5	0	5.8	10.6	1.9	4.6	−1.1	0.35
Ridge Glacier	20	0.8	0	3.6	11.3	1.9	8.9	−1.8	0.39
Salisbury Glacier	23	3.2	0	10.8	9.3	3.1	14.6	−3.3	0.45
Scott Glacier	153	0.4	0	8.4	11.3	2.6	10.0	−2.6	0.41
Sladden Glacier	125	1.7	0	4.7	12.5	2.0	6.9	−1.9	0.35
Spa Glacier	141	1.3	0	10.9	9.4	3.1	10.6	−2.8	0.49
Spencer Glacier	105	11.7	10	9.9	9.8	2.5	4.6	−2.2	0.44
Strauchon Glacier	104	4.2	17	9.3	11.0	2.4	3.4	−2.3	0.25
Tasman Glacier	22	101.1	30	7.6	10.7	1.8	3.6	−1.5	0.30
Tekano Glacier	155	0.7	0	8.0	11.4	2.6	11.5	−2.3	0.41
Tewaewae Glacier	124	0.7	0	6.1	11.9	2.7	11.9	−2.7	0.35
Victoria Glacier	113	6.2	13	10.7	9.7	2.7	4.9	−2.7	0.38
Whymper Glacier	106	12.7	27	8.7	10.2	1.9	3.9	−2.0	0.26

[a]Geometric data are based on topographic mapping undertaken in 1986; glacier area includes all ice within the catchment of nonindex glaciers. Precipitation is averaged over the area of the glacier.
[b]Continentality, defined as the difference between the mean temperature of the warmest and coolest months, is averaged over the area of the glacier.
[c]Temperature sensitivity is to a 1 K change.
[d]Precipitation sensitivity is to a 10% change.

were not as well simulated at Tasman Glacier. This result is not surprising given the very similar climatic and glaciological settings of Fox and Franz Josef glaciers (high rainfall, high melt, low-elevation measurement sites), and the lower-precipitation and higher-elevation Tasman Glacier sites. The issue of equifinality was also highlighted by the model sensitivity analysis which showed that different parameter choices could not be adequately discriminated between based on the existing mass balance data set.

[49] The main results presented here are related to mass balance sensitivity, rather than mass balance itself. Mass balance sensitivity is a function of the climatic and glaciological setting, but because it is calculated as a difference between model simulations the values are less sensitive to model error than the mass balance output. This is because the model error largely subtracts out between the perturbed and unperturbed calculations. However, where parameter values influence the mass turnover, such as for temperature lapse rate and snow/rain threshold temperature, there is some

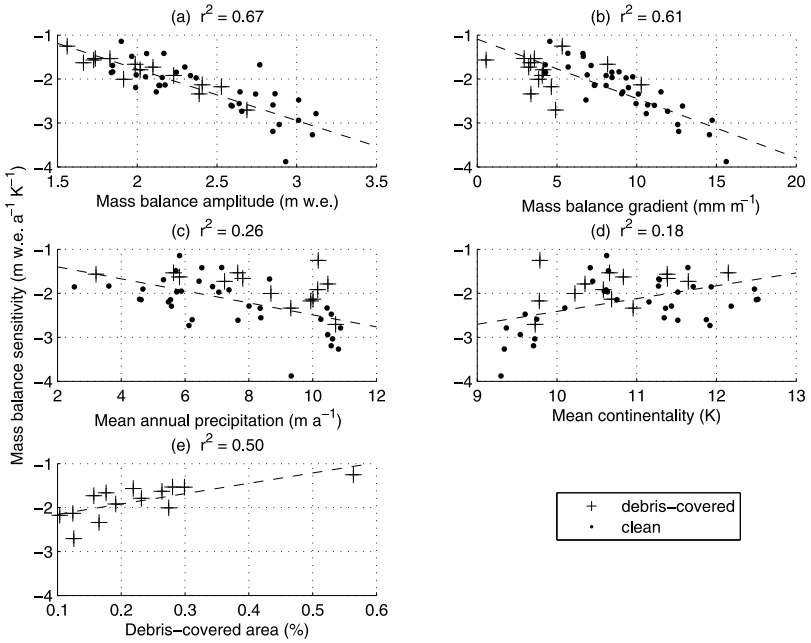

Figure 7. The sensitivity of glacier mass balance to temperature changes of 1 K versus (a) mass balance amplitude, (b) mass balance gradient, (c) area-averaged precipitation, (d) area-averaged continentality, and (e) proportion of debris-covered area, calculated using the full-energy balance model.

uncertainty in the absolute values of the mass balance sensitivity (Figure 5). Despite this uncertainty, the spatial patterns in mass balance sensitivity do not change. The mass balance and sensitivity simulations on Fox, Franz Josef and Tasman glaciers are robust and, as the model has been tested outside of the calibration site and time, we infer that mass balance sensitivity on unmeasured glaciers is also well represented by the model.

6.2. Magnitude of Mass Balance Sensitivity

[50] Recent work [*Braithwaite and Raper*, 2007; *Hock et al.*, 2009; *De Woul and Hock*, 2005] has shown that the range of mass balance sensitivities in nature is much wider than previously thought [*Braithwaite et al.*, 2003; *Oerlemans and Fortuin*, 1992], although *Oerlemans* [2005] calculates very high sensitivities for some glaciers [*Oerlemans,* 2005, Figure S2]. This study shows that sensitivities in the maritime

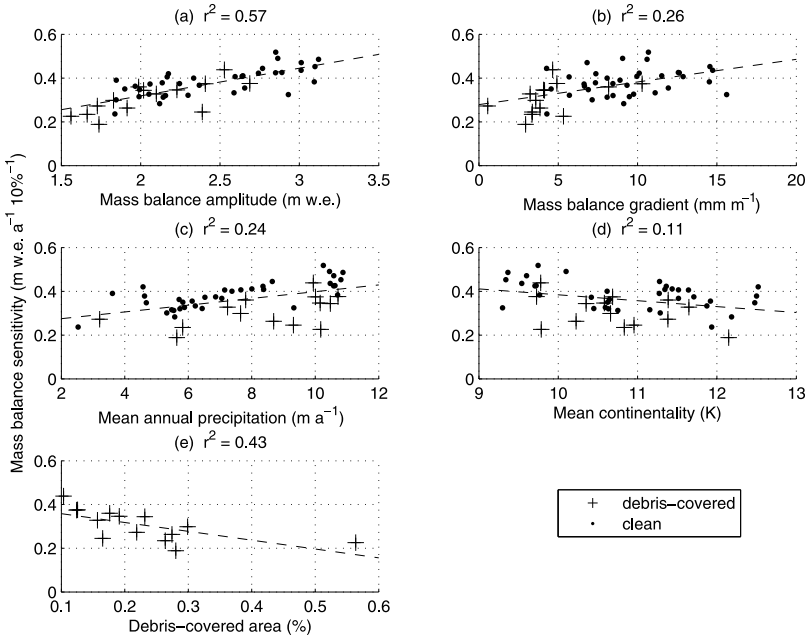

Figure 8. The sensitivity of glacier mass balance to precipitation changes of 10% versus (a) mass balance amplitude, (b) mass balance gradient, (c) area-averaged precipitation, (d) area-averaged continentality, and (e) proportion of debris-covered area, calculated using the full-energy balance model.

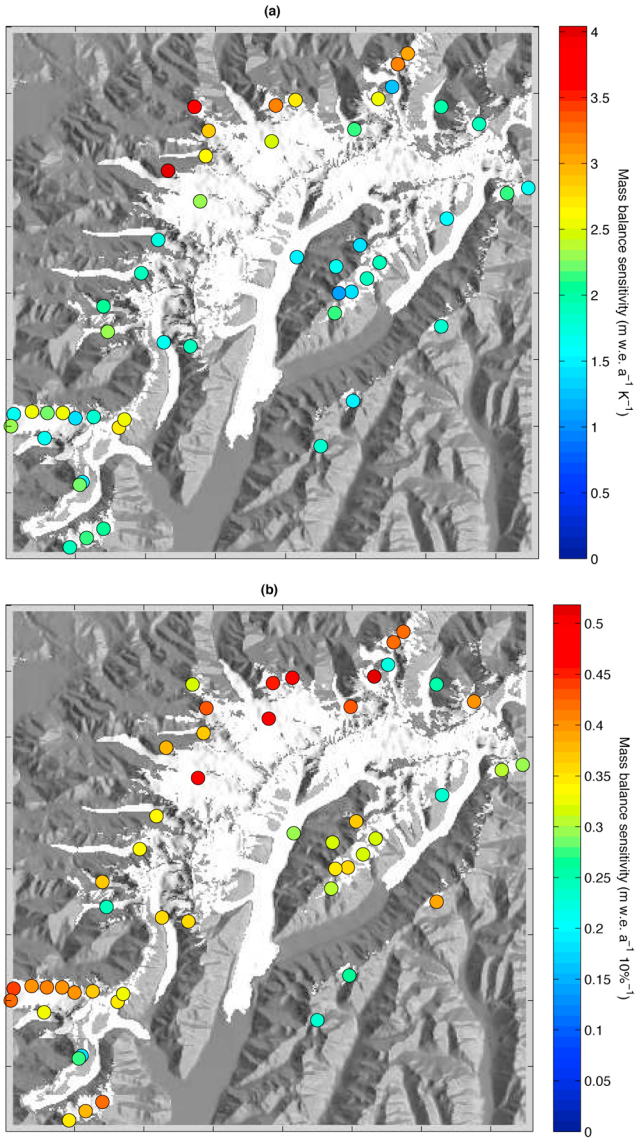

Figure 9. Spatial pattern of mass balance (a) temperature and (b) precipitation sensitivity in the central Southern Alps. Each circle is plotted at the centroid of a glacier, and the color indicates the magnitude of mass balance sensitivity. For scale, ticks on the axes are at 5 km intervals.

Southern Alps also have a wide range, with values in the range −1.1 to −4.0 m w.e. a^{-1} K^{-1} . The overall sensitivity of glaciers of the central Southern Alps, calculated at −1.9 m w.e. a^{-1} K^{-1} corresponds well to the value of −1.87 m w.e. a^{-1} K^{-1} calculated by *Braithwaite and Raper* [2007] using global gridded climate surfaces and glacier inventory data.

[51] The most sensitive glaciers in our analysis are those which are located about midway up the mountain slope of the Southern Alps on the windward side of the drainage divide. This is the region of peak precipitation, 5–10 km southeast of the Alpine Fault [*Henderson and Thompson*, 1999], with ∼10 m a^{-1} area-averaged precipitation at Salisbury Glacier and ∼9 m a^{-1} at Jalf Glacier. These precipitation values are well outside the 0–5 m/a range described by *Braithwaite et al.* [2003], *Oerlemans* [2001], and *Oerlemans and Fortuin* [1992] which explains why the sensitivities are so high.

[52] The spatial pattern of sensitivity (Figure 9) allows an assessment of the hypothesis that there is a strong gradient in sensitivity, increasing from east to west as a result of the climatic gradients across the Southern Alps. As suggested by the relationships between precipitation and continentality versus sensitivity (Figures 7 and 8) there is only a weak relationship for temperature sensitivity, but there is a strong pattern for precipitation sensitivity. This result indicates that our initial hypothesis, that there is a reduction in mass balance sensitivity from west to east as a result of decreasing precipitation, is only weakly supported and that topographic effects play a significant role in determining mass balance sensitivity, especially to temperature.

6.3. Controls on Mass Balance Sensitivity

[53] Previous work has related mass balance sensitivities to mass balance amplitude [*Braithwaite et al.*, 2003; *Meier*, 1984], precipitation [*Oerlemans and Fortuin*, 1992; *Oerlemans*, 1992], or continentality index [*Holmlund and Schneider*, 1996; *De Woul and Hock*, 2005; *Hock et al.*, 2009] with more sensitive glaciers found in maritime environments. Before we consider how the results of this study help elucidate these relationships, we first discuss how climatic and topographic characteristics could be expected to influence mass balance sensitivity.

[54] That glaciers with a higher mass turnover are more sensitive to climatic changes has long been recognized [*Meier*, 1984], but the relationship was not explored in detail until *Braithwaite and Zhang* [1999]. However, it is not high turnover itself that makes glaciers sensitive, rather the factors that lead to high turnover also lead to high sensitivity.

[55] High precipitation is a necessary, but not sufficient condition for high mass turnover. This follows from equation (11); for a glacier in equilibrium $b_w = -b_s$ and a high b_w can only occur when precipitation is high. However, on low-elevation glaciers the proportion of precipitation that falls as snow may be small. Alternatively the accumulation area might be restricted providing a limit on the area-averaged winter balance b_w. Examples from the Southern Alps data set illustrate these points. Burton Glacier has an area-averaged annual precipitation of >10 m a^{-1}, but a relatively low mass balance amplitude of 1.6 m w.e. (Table 4). In this case the accumulation area is small relative to the disproportionately large ablation area which results from a surface debris cover of ∼55%. Another example is Gulch Glacier which has a mean annual precipitation of ∼10 m a^{-1} and a mass balance amplitude of 2.4 m w.e. In this case the mass balance amplitude is not retarded by significant debris cover, which is 12% on this glacier, but rather because of the glacier's steep surface slope. The glaciers with highest mass balance amplitude (Spa, Salisbury, Fritz, Chancellor and Jalf) are all in the peak precipitation band (Table 4). Precipitation is the principal control on mass balance amplitude, but it is confounded by topographic effects which we have identified in this study.

[56] It is not possible to separate the influences of precipitation and continentality on mass balance sensitivity as areas with high continentality tend to also have low precipitation [*Braithwaite*, 2005; *Oerlemans*, 2001]. Analysis of the seasonal variation of sensitivity [*Oerlemans and Reichert*, 2000]

shows that annual sensitivity is a combination of monthly components, and that these monthly components vary in different climatic environments. Continentality influences temperature sensitivity because the part of the year when temperatures are warm enough to cause melt, and therefore sensitivity of ablation to temperature, is limited in continental environments while melt occurs year-round in highly maritime environments. The fraction of precipitation that falls as snow is also highly dependent on temperature in maritime environments as the temperature is often close to the snow/rain threshold and small changes in temperature result in a large change in the partitioning of precipitation into rain or snow.

[57] There are four main ways that sensitivity can be controlled by topographic factors: (1) aspect: on shady or oblique slopes a larger proportion of the energy available for melt is supplied by turbulent heat fluxes which are sensitive to temperature, (2) slope: glaciers with low slope angles are more susceptible to large variations in mass balance because changes in the partitioning of precipitation into rain and snow result in changes over a large fraction of the glacier [*Anderson et al.*, 2010], (3) elevation: glaciers that extend to lower elevations have a longer melt season, and melt increases nonlinearly with increasing temperature [*Oerlemans and Fortuin*, 1992], and (4) debris cover: glaciers with significant debris cover have retarded ablation and hence a lower sensitivity to temperature.

[58] Given the previous discussion, it is surprising that there is no clear relationship between any of the climatic or topographic characteristics and mass balance sensitivity, with the exception of debris cover. The strong relationship between mass turnover and sensitivity gives some confidence that the model is giving a reliable indication of the mass balance regime, and we conclude that there is no simple relationship. While previous work has related overall mass balance sensitivity to precipitation [*Oerlemans and Fortuin*, 1992] or accumulation sensitivity to precipitation and ablation sensitivity to continentality [*Hock et al.*, 2009] the underlying relationships, despite having a good physical basis, are similarly weak [*Hock et al.*, 2009, Figure S2; *Oerlemans and Fortuin*, 1992, Figure 3]. Fortunately we have demonstrated that the relationship between mass balance amplitude and sensitivity is robust, a similar finding to that of *Braithwaite et al.* [2003].

[59] Calculating mass balance amplitude using an energy balance or degree-day model is a detailed undertaking which requires good quality information on the topographic and climatic setting of each glacier. Such topographic information is becoming available through the Global Land Ice Measurement from Space program (GLIMS) [*Raup et al.*, 2007]. Global climatic information is available through reanalysis data [*Kalnay et al.*, 1996; *Uppala et al.*, 2005]. Together the topographic and climatic data will eventually provide an opportunity to explicitly calculate glacier sensitivity on a global scale.

[60] However this study highlights another possibility, i.e., to parameterize mass balance sensitivity using the mass balance gradient, which is strongly related to both temperature and precipitation sensitivity (Figures 7b and 8b). The advantage of using mass balance gradient over mass balance amplitude is that hypsometric information is not required, an important distinction given that the existing World Glacier Inventory [*National Snow and Ice Data Center*, 1999] does not generally contain hypsometric information. A simple degree-day or energy balance model is sufficient. The advantage of this simpler approach is that it is feasible to calculate mass balance gradients on a global scale using gridded climatological data [*New et al.*, 2002] or reanalysis data [*Kalnay et al.*, 1996; *Uppala et al.*, 2005] and the limited topographic information that is contained in existing glacier inventories. Based on our findings this approach should provide a robust calculation of glacier sensitivity. In particular the approach can account for the effect of surface debris cover on glacier response, an important consideration in many mountain ranges on Earth, especially where rates of tectonic uplift are high, for example the Himalaya and Karakoram.

7. Conclusion

[61] By using a detailed energy balance model applied to glaciers in the central portion of the Southern Alps of New Zealand we have identified the variations in mass balance sensitivity of these glaciers. Sensitivities vary between -1.1 m w.e. K^{-1} and -4.0 m w.e. a^{-1} K^{-1}. The highest values are for two small, low-angle glaciers in the high-precipitation band west of the main divide. This study has added to the data set for the maritime half of the sensitivity spectrum [*Braithwaite et al.*, 2003].

[62] The absolute values of mass balance sensitivity were found depend to some extent on parameter choice, especially temperature lapse rate and the snow/rain threshold. These results point to the need for more mass balance and climatic data collection across the climatic gradients of the Southern Alps in order to better understand the differences in climatic and glaciological setting, with emphasis on lapse rate and accumulation measurement. Despite this limitation, the pattern of mass balance sensitivity derived in this study was found to be relatively insensitive to model parameter choices.

[63] Taken alone, climatic measures such as mean annual precipitation and continentality were found to be poor predictors of mass balance sensitivity. Topographic characteristics such as surface slope, aspect and elevation range were also discovered to be poor predictors. The only topographic or climatic characteristic that was directly related to sensitivity is surface debris cover. The impact of debris cover on glacier sensitivity does not appear to have been addressed before, but it was found to reduce sensitivity significantly. This is because on the debris-covered portion of the glacier, ablation is retarded so the impact of temperature on melt is similarly reduced. Glaciers with higher proportions of debris cover are less sensitive to both temperature and precipitation changes.

[64] Mass balance amplitude is inherently linked to climatic sensitivity, where glaciers with higher mass balance amplitude are also more sensitive to both temperature and precipitation changes. Our results show that the mass balance gradient of a glacier is closely related to its mass balance amplitude and is almost as good a predictor of mass balance sensitivity. Climatic characteristics are the fundamental control on mass balance gradient, but this control is also influenced by debris cover which, in this analysis, is the only topographic characteristic that systematically influences

the mass balance gradient. In particular we conclude that glacier hypsometry only has a secondary effect on climatic sensitivity. This finding indicates that the sensitivity of glaciers can be calculated efficiently by using a simplified degree-day or energy balance model on simplified glacier geometry as, for example, is contained in glacier inventories, taking into account debris cover where appropriate. Such an approach would be an improvement on the current methods of interpolating mass balance sensitivities from a few well known glaciers and will reduce the uncertainties associated with calculating the glacier and small ice cap contribution to sea level rise estimates [*Hock et al.*, 2009].

[65] The inclusion of debris cover in global estimates of glacier sensitivity is likely to slightly reduce the average global sensitivity, and therefore the magnitude of sea level rise in the coming century especially because the area of glacier surface which is debris covered is increasing [e.g., *Bolch et al.*, 2008]. This reduced sensitivity might be countered by the fact that heavily debris covered glaciers have a tendency to down-waste vertically rather than retreat horizontally, making them prone to lake calving retreat [*Kirkbride and Warren*, 1999]. This means that although the static sensitivity of debris-covered glaciers is smaller than previously estimated, the response of these glaciers to warming may actually be amplified by dynamic retreat due to lake calving, a process underway in many mountain ranges including the Southern Alps of New Zealand.

[66] **Acknowledgments.** We thank Roger Braithwaite, one anonymous reviewer, and the Associate Editor for their detailed and constructive reviews which have significantly improved this paper. The authors were supported by the Comer Science and Education Fund and FRST contracts ANZICE and NIWA Regional Climate Modeling. We thank Fox Glacier Guides and Heather Purdie, who collected mass balance data for Fox and Tasman glaciers, respectively, and Franz Josef Glacier Guides who have supported data collection on Franz Josef Glacier for many years. Access to these National Park and World Heritage areas is an integral part of this work, and we appreciate the support of the Department of Conservation in granting access. NCEP Reanalysis data were provided by the NOAA/OAR/ESRL PSD, Boulder, Colorado, USA, from their Web site at http://www.esrl.noaa.gov/psd/.

References

Anderson, B. M., and A. N. Mackintosh (2006), Temperature change is the major driver of late-glacial and Holocene glacier fluctuations in New Zealand, *Geology*, *34*(2), 121–134, doi:10.1130/G22151.1.

Anderson, B. M., W. J. Lawson, I. F. Owens, and B. Goodsell (2006), Past and future mass balance of "Ka Roimata o Hine Hukatere" Franz Josef Glacier, New Zealand, *J. Glaciol.*, *52*, 597–607, doi:10.3189/172756506781828449.

Anderson, B. M., W. J. Lawson, and I. F. Owens (2008), Response of Franz Josef Glacier Ka Roimata o Hine Hukatere to climate change, *Global Planet. Change*, *63*, 23–30, doi:10.1016/j.gloplacha.2008.04.003.

Anderson, B. M., A. N. Mackintosh, D. Stumm, L. George, T. Kerr, A. Winter-Billington, and S. J. Fitzsimons (2010), Climate sensitivity of a high-precipitation glacier in New Zealand, *J. Glaciol.*, *56*, 114–128, doi:10.3189/002214310791190929.

Arendt, A. A., K. A. Echelmeyer, W. D. Harrison, C. S. Lingle, and V. B. Valentine (2002), Rapid wastage of Alaska glaciers and their contribution to rising sea level, *Science*, *297*, 382–386, doi:10.1126/science.1072497.

Barringer, J. R. F. (1989), A variable lapse rate snowline model for the Remarkables, central Otago, New Zealand, *N. Z. J. Hydrol.*, *28*, 32–46.

Berthier, E., E. Schiefer, G. K. C. Clarke, B. Menounos, and F. Remy (2010), Contribution of Alaskan glaciers to sea-level rise derived from satellite imagery, *Nat. Geosci.*, *3*(2), 92–95, doi:10.1038/ngeo737.

Bolch, T., M. F. Buchroithner, T. Pieczonka, and A. Kunert (2008), Planimetric and volumetric glacier changes in the Khumbu Himal, Nepal, since 1962 using Corona, Landsat TM and ASTER data, *J. Glaciol.*, *54*, 592–600, doi:10.3189/002214308786570782.

Braithwaite, R. J. (1985), Calculation of degree days for glacier climate research, *Z. Gletscherkd. Glazialgeol.*, *20*, 1–8.

Braithwaite, R. J. (2005), Mass-balance characteristics of arctic glaciers, *Ann. Glaciol.*, *42*, 225–229, doi:10.3189/172756405781812899.

Braithwaite, R. J. (2008), Temperature and precipitation climate at the equilibrium-line altitude of glaciers expressed by the degree-day factor for melting snow, *J. Glaciol.*, *54*, 437–444, doi:10.3189/002214308785836968.

Braithwaite, R. J., and S. C. B. Raper (2007), Glaciological conditions in seven contrasting regions estimated with the degree-day model, *Ann. Glaciol.*, *46*, 297–302, doi:10.3189/172756407782871206.

Braithwaite, R. J., and Y. Zhang (1999), Modelling changes in glacier mass balance that may occur as a result of climate changes, *Geogr. Ann., Ser. A*, *81*(4), 489–496, doi:10.1111/j.0435-3676.1999.00078.x.

Braithwaite, R. J., Y. Zhang, and S. C. B. Raper (2003), Temperature sensitivity of the mass balance of mountain glaciers and ice caps as a climatological characteristic, *Z. Gletscherkd. Glazialgeol.*, *38*(1), 35–61.

Calov, R., and R. Greve (2005), Correspondence: A semi-analytical solution for the positive degree-day model with stochastic temperature variations, *J. Glaciol.*, *51*, 173–175.

Chinn, T. J. (1989), Glaciers of New Zealand, *U.S. Geol. Surv. Prof. Pap.*, *1386-H-2*.

Chinn, T. J. (1999), New Zealand glacier response to climate change of the past 2 decades, *Global Planet. Change*, *22*, 155–168, doi:10.1016/S0921-8181(99)00033-8.

Chinn, T. J. (2001), Distribution of the glacial water resources of New Zealand, *N. Z. J. Hydrol.*, *40*, 139–187.

Cogley, J. G. (2009), Geodetic and direct mass-balance measurements: Comparison and joint analysis, *Ann. Glaciol.*, *50*, 96–100, doi:10.3189/172756409787769744.

Corripio, J. G. (2003), Vectorial algebra algorithms for calculating terrain parameters from DEMs and solar radiation modelling in mountainous terrain, *Int. J. Geogr. Inf. Sci.*, *17*, 1–23, doi:10.1080/713811744.

De Woul, M., and R. Hock (2005), Static mass-balance sensitivity of Arctic glaciers and ice caps using a degree-day approach, *Ann. Glaciol.*, *42*, 217–224, doi:10.3189/172756405781813096.

Dyurgerov, M. B., and M. F. Meier (2000), Twentieth century climate change: Evidence from small glaciers, *Proc. Natl. Acad. Sci. U. S. A.*, *97*(4), 1406–1411, doi:10.1073/pnas.97.4.1406.

Elsberg, D. H., W. D. Harrison, K. A. Echelmeyer, and R. M. Krimmel (2001), Quantifying the effects of climate and surface change on glacier mass balance, *J. Glaciol.*, *47*, 649–658, doi:10.3189/172756501781831783.

Furbish, D. J., and J. T. Andrews (1984), The use of hypsometry to indicate long-term stability and response of valley glaciers to changes in mass transfer, *J. Glaciol.*, *30*, 199–211.

Henderson, R. D., and S. M. Thompson (1999), Extreme rainfalls in the Southern Alps of New Zealand, *N. Z. J. Hydrol.*, *38*, 309–330.

Hessell, J. W. D. (1980), Apparent trends of mean temperature in New Zealand since 1930, *N. Z. J. Sci.*, *23*, 1–9.

Hock, R. (2005), Glacier melt: A review of processes and their modelling, *Prog. Phys. Geogr.*, *29*(3), 362–391, doi:10.1191/0309133305pp453ra.

Hock, R., M. de Woul, V. Radić, and M. Dyurgerov (2009), Mountain glaciers and ice caps around Antarctica make a large sea-level rise contribution, *Geophys. Res. Lett.*, *36*, L07501, doi:10.1029/2008GL037020.

Hoelzle, M., T. Chinn, D. Stumm, F. Paul, M. Zemp, and W. Haeberli (2007), The application of glacier inventory data for estimating past climate change effects on mountain glaciers: A comparison between the European Alps and the Southern Alps of New Zealand, *Global Planet. Change*, *56*, 69–82.

Holmlund, P., and T. Schneider (1996), The effect of continentality on glacier response and mass balance, *Ann. Glaciol.*, *24*, 272–276.

Johannesson, T. J., O. Sigursson, T. Laumann, and M. Kennett (1995), The response of two Icelandic glaciers to climatic warming computed with a degree-day glacier mass balance model coupled to a dynamic glacier model, *J. Glaciol.*, *43*, 345–358.

Kalnay, E., et al. (1996), The NCEP/NCAR 40-Year Reanalysis Project, *Bull. Am. Meteorol. Soc.*, *77*, 437–471, doi:10.1175/1520-0477(1996)077<0437:TNYRP>2.0.CO;2.

Kaser, G., J. G. Cogley, M. B. Dyurgerov, M. F. Meier, and A. Ohmura (2006), Mass balance of glaciers and ice caps: Consensus estimates for 1961–2004, *Geophys. Res. Lett.*, *33*, L19501, doi:10.1029/2006GL027511.

Kees, L. (2011), Snow storage gradient across a maritime mountain range: A GPR assessment, M.S. thesis, Victoria Univ. of Wellington, Wellington, New Zealand.

Kirkbride, M. P. (1989), The influence of sediment budget on geomorphic activity of the Tasman Glacier, Mount Cook National Park, Ph.D. thesis, Univ. of Canterbury, Christchurch, New Zealand.

Kirkbride, M. P., and C. R. Warren (1999), Tasman Glacier, New Zealand: 20th-century thinning and predicted calving retreat, *Global Planet. Change*, *22*, 11–28, doi:10.1016/S0921-8181(99)00021-1.

MacDougall, A. H., B. A. Wheler, and G. E. Flowers (2010), Assessment of glacier melt-model transferability: Comparison of temperature-index and energy-balance models, *Cryosphere Discuss.*, *4*(4), 2143–2167, doi:10.5194/tcd-4-2143-2010.

Meier, M. F. (1984), Contribution of small glaciers to global sea level, *Science*, *226*, 1418–1421, doi:10.1126/science.226.4681.1418.

Moore, R. D., and I. F. Owens (1984), Modelling alpine snow accumulation and ablation using daily climate observations, in *Proceedings of the 12th Conference of the New Zealand Geographical Society*, pp. 88–92, N. Z. Geogr. Soc., Christchurch, New Zealand.

National Snow and Ice Data Center (1999), World Glacier Inventory, http://nsidc.org/data/g01130.html, Boulder, Colo.

Neale, S. M., and B. B. Fitzharris (1997), Energy balance and synoptic climatology of a melting snowpack in the Southern Alps, New Zealand, *Int. J. Climatol.*, *17*, 1595–1609, doi:10.1002/(SICI)1097-0088(19971130)17:14<1595::AID-JOC213>3.0.CO;2-7.

New, M., D. Lister, M. Hulme, and I. Makin (2002), A high-resolution data set of surface climate over global land areas, *Clim. Res.*, *21*(1), 1–25, doi:10.3354/cr021001.

Oerlemans, J. (1989), On the response of valley glaciers to climatic change, in *Glacier Fluctuations and Climatic Change: Proceedings of the Symposium on Glacier Fluctuations and Climatic Change, Held in Amsterdam, 1–5 June 1987*, pp. 353–371, Kluwer Acad., Dordrecht, Netherlands.

Oerlemans, J. (1992), Climate sensitivity of glaciers in southern Norway: Application of an energy balance model to Nigardsbreen, Hellstugubreen, and Alfotbreen, *J. Glaciol.*, *38*, 223–232.

Oerlemans, J. (1997a), A flowline model for Nigardsbreen, Norway: Projection of future glacier length based on dynamic calibration with the historic record, *Ann. Glaciol.*, *24*, 382–389.

Oerlemans, J. (1997b), Climate sensitivity of Franz Josef Glacier, New Zealand, as revealed by numerical modelling, *Arct. Alp. Res.*, *29*(2), 233–239, doi:10.2307/1552052.

Oerlemans, J. (2001), *Glaciers and Climate Change*, A. A. Balkema, Rotterdam, Netherlands.

Oerlemans, J. (2005), Extracting a climate signal from 169 glacier records, *Science*, *308*, 675–677, doi:10.1126/science.1107046.

Oerlemans, J., and J. P. F. Fortuin (1992), Sensitivity of glaciers and small ice caps to greenhouse warming, *Science*, *258*, 115–117, doi:10.1126/science.258.5079.115.

Oerlemans, J., and W. H. Knap (1998), A 1 year record of global radiation and albedo in the ablation zone of Morteratschgletscher, Switzerland, *J. Glaciol.*, *44*, 231–238.

Oerlemans, J., and B. K. Reichert (2000), Relating glacier mass balance to meteorological data by using a seasonal sensitivity characteristic, *J. Glaciol.*, *46*, 1–6, doi:10.3189/172756500781833269.

Oerlemans, J., R. P. Bassford, W. Chapman, J. A. Dowdeswell, A. F. Glazovsky, J. O. Hagen, K. Melvold, M. de Ruyter de Wildt, and R. S. W. van de Wal (2005), Estimating the contribution of Arctic glaciers to sea-level change in the next 100 years, *Ann. Glaciol.*, *42*, 230–236, doi:10.3189/172756405781812745.

Ohmura, A., P. Kasser, and M. Funk (1992), Climate at the equilibrium line of glaciers, *J. Glaciol.*, *38*, 397–411.

Paterson, W. S. B. (1994), *The Physics of Glaciers*, 3rd ed., Pergamon, Oxford, U. K.

Purdie, J., and B. Fitzharris (1999), Processes and rates of ice loss at the terminus of Tasman Glacier, New Zealand, *Global Planet. Change*, *22*, 79–91, doi:10.1016/S0921-8181(99)00027-2.

Raper, S. C. B., and R. J. Braithwaite (2006), Low sea level rise projections from mountain glaciers and icecaps under global warming, *Nature*, *439*(7074), 311–313, doi:10.1038/nature04448.

Rasmussen, L. A., and H. Conway (2005), Influence of upper-air conditions on glaciers in Scandinavia, *Ann. Glaciol.*, *42*, 402–408, doi:10.3189/172756405781812727.

Raup, B., A. Racoviteanu, S. J. S. Khalsa, C. Helm, R. Armstrong, and Y. Arnaud (2007), The GLIMS geospatial glacier database: A new tool for studying glacier change, *Global Planet. Change*, *56*, 101–110, doi:10.1016/j.gloplacha.2006.07.018.

Ruddell, A. R. (1995), Recent glacier and climate change in the New Zealand Alps, Ph.D. thesis, Univ. of Melbourne, Melbourne, Victoria, Australia.

Salinger, M. J., M. J. Heine, and C. J. Burrows (1983), Variations of the Stocking (Te Wae Wae) Glacier, Mount Cook and climatic relationships, *N. Z. J. Sci.*, *26*, 321–338.

Salinger, M. J., J. E. Hay, R. McGann, and B. B. Fitzharris (1993), Southwest Pacific temperatures: Diurnal and seasonal trends, *Geophys. Res. Lett.*, *20*, 935–938, doi:10.1029/93GL01113.

Stuart, S. J. (2011), Observations and modelling of precipitation in the Southern Alps of New Zealand, M.S. thesis, Victoria Univ. of Wellington, Wellington, New Zealand.

Suggate, R. P. (1952), Franz Josef Glacier, March 1951, *N. Z. J. Sci. Technol.*, *33*(4), 299–304.

Tait, A., R. Henderson, R. Turner, and X. Zheng (2006), Thin plate smoothing spline interpolation of daily rainfall for New Zealand using a climatological rainfall surface, *Int. J. Climatol.*, *26*, 2097–2115, doi:10.1002/joc.1350.

Uppala, S. M., et al. (2005), The ERA-40 re-analysis, *Q. J. R. Meteorol. Soc.*, *131*, 2961–3012, doi:10.1256/qj.04.176.

Warren, C. R., and M. P. Kirkbride (2003), Calving speed and climatic sensitivity of New Zealand lake-calving glaciers, *Ann. Glaciol.*, *36*, 173–178, doi:10.3189/172756403781816446.

B. Anderson and A. Mackintosh, Antarctic Research Centre, Victoria University of Wellington, PO Box 600, Wellington 6140, New Zealand. (brian.anderson@vuw.ac.nz; andrew.mackintosh@vuw.ac.nz)